

**Anomalous thermal transport in disordered harmonic chains and carbon nanotubes**

Xiaoxi Ni, Meng Lee Leek, Jian-Sheng Wang, and Yuan Ping Feng  
*Department of Physics and Center for Computational Science and Engineering,  
 National University of Singapore, Singapore 117542, Singapore*

Baowen Li  
*Department of Physics and Center for Computational Science and Engineering,  
 National University of Singapore, Singapore 117542, Singapore and  
 NUS Graduate School for Integrative Sciences and Engineering, Singapore 117456, Singapore*  
 (Received 21 April 2010; revised manuscript received 29 September 2010; published 21 January 2011)

We report the coherent potential approximation method of treating quantum thermal transport properties of nanoscale systems with mass disorder. Instead of massive efforts required in brute-force calculations, configuration averaging of disordered systems can be efficiently handled in a self-consistent manner by setting up the phonon version of nonequilibrium vertex correction theory. The accuracy of the method is verified by comparing with the exact results and Monte Carlo experiments in one-dimensional atomic chains. Results obtained for disordered harmonic chains and carbon nanotubes provide evidence of anomalous thermal transport in such systems. We also observe crossover in the transport where phonon scattering by disorder becomes important. Our results show that disorder plays a role in thermal conductance reduction.

DOI: [10.1103/PhysRevB.83.045408](https://doi.org/10.1103/PhysRevB.83.045408)

PACS number(s): 63.20.kp, 65.80.Ck, 66.70.Df

**I. INTRODUCTION**

Recent years have witnessed a renaissance of interest in studying matter that is disordered in either composition or structure, because the intentional incorporation of atomic impurities is routinely used to control and manipulate the electrical, thermal, optical, and magnetic properties of semiconductors. For example, the long-range electrostatic potential due to charged dopants can lead to a dramatic suppression of minority carriers.<sup>1</sup> Thermal conductivity of silicon nanowires can be reduced exponentially by isotopic disorder;<sup>2</sup> spin scattering by disorder can invert magnetoresistance in magnetic nanojunctions.<sup>3</sup> When an experiment is carried out to measure a physical quantity of a sample in a particular configuration of disorder, only the average trend of that quantity is of interest. Since disorder configurations can be taken to be random, the average trend of the measured physical quantities is found by averaging over all possible configurations. If one carries out this average by randomly generating a configuration for a given concentration  $C$  of disorder and averaging the resulting physical quantity for a large sample of configurations, it is neither worth the computational effort when  $C$  is small nor practical owing to the possibilities of misleading errors when it comes to relatively large systems, like carbon nanotubes, or systems with a large surface-to-volume ratio. This is because the transport quantities are not quite similar when the dopants are found at the surface or in the bulk.

Enormous efforts were made<sup>4</sup> in the 1970s to derive better approximation methods in order to carry out the configurational average. The brute-force method of configuration averaging is obviously not preferred because a large number of configurations exist. For example, we consider a substitutionally disordered binary alloy with  $N$  sites; there are  $2^N$  configurations. One of the most important approximation methods is the introduction of the coherent potential approximation<sup>5</sup> (CPA) for treating elementary excitations

in disordered systems. However, the CPA has only been applied to near-equilibrium electronic and thermal transport calculations; in view of today's nanodevices that operate far from equilibrium, the full nonequilibrium description is required. Recently, the so-called nonequilibrium vertex correction<sup>6</sup> (NVC) theory was derived based on the CPA to calculate the atomistic nonequilibrium configurational average of a two-particle Green's function, which is required to evaluate the quantum electronic transport problem. In order to complete this scheme, we here report the results of the analogous quantum thermal transport problem. Since the CPA is applied to regimes where conventional perturbation theory is not directly accessible, we will comment on its accuracy based on the number of moments of the density of states (DOS) exactly reproduced. For diagonal disorder, CPA reproduces exactly seven moments of the average DOS.<sup>7</sup> It is also noteworthy that the inverse coordination number  $Z^{-1}$  seems to be a suitable small parameter to perturbatively probe those inaccessible regimes defined by other parameters.<sup>8</sup>

The organization of the paper is as follows: In Sec. II, we will first introduce briefly the mass impurity model and the notion and notation of configuration averaging. We will then incorporate configuration averaging into the quantum dynamics and impose the CPA to get a self-consistent relation. The retarded single-particle Green's function is calculated in this way. The Caroli formula,<sup>16</sup> derived from the nonequilibrium Green's function formalism (NEGF), is the nonequilibrium quantity that we use to calculate the transport properties. The extra step is to impose the CPA and configuration averaging. To carry out this step, we need the thermal transport version of NVC. Proceeding to Sec. III, we first compare the case in short one-dimensional (1D) atomic chains where exact results can be evaluated by averaging over every possible configuration. We show that the larger the system is, the more accurate the theoretical value is. Section IV follows with the results of implementing the theory on 1D mass-disordered harmonic

chains. The result shows that the behavior of the thermal conductivity  $\kappa$  with increasing system size is significantly affected by the properties of the heat bath. As a special case, we recover the earlier result<sup>9-11</sup> that gave  $\kappa \sim N^{\frac{1}{2}}$  for the free-boundary condition. Other cases where we add an extremely small pinning on the first and last atoms give rise to a turning point and change the power law behavior. This size effect indicates that the exponent may not necessarily be a constant under a fixed number of pinning potential centers. This is unlike the argument predicted previously:  $\kappa \sim N^{-n+\frac{3}{2}}$ , where  $n \geq 2$  is the number of pinning centers.<sup>13</sup> Finally, in Sec. V, the theory is employed to study the effect of isotope disorder on the thermal transport properties of carbon nanotubes, one of most promising nanoscale materials discovered in the past decade. Much theoretical and experimental work has been done to predict their thermal properties.<sup>14,15</sup> As a possible application of this theory, we attempt to address the outstanding issue of how impurity dopants affect the transition from ballistic thermal transport to superdiffusive thermal transport.

## II. FORMALISM AND MODEL

We consider a central scattering region sandwiched by two semi-infinite thermal leads. The two leads serve as heat baths providing a temperature difference across the central region and the two leads are uncorrelated. The Hamiltonian of the full model is given as

$$H = H^L + H^{LC} + H^C + H^{CR} + H^R, \quad (1)$$

where  $H^L$  and  $H^R$  are the terms representing the left and right semi-infinite harmonic heat baths.  $H^{LC}$  and  $H^{CR}$  are the terms for the linear couplings of the central region to the leads. For the explicit form of these terms, see Ref. 16. Here, we will simply incorporate the effects of the leads using the NEGF-derived<sup>16</sup> form of the Landauer formalism.  $H^C$  is the term for the mass-disordered central region in the harmonic approximation.

### A. Configurational average

Note that we assume that impurities only exist inside the central scattering region and not in the left or right leads. Any atomic position (degree of freedom)  $s$  in the scattering region may be occupied by one of the two atomic species  $Q = A, B$  with concentration or probability  $C_s^A$  and  $C_s^B$  such that  $C_s^A + C_s^B = 1$ .

For any quantity  $X_s$  defined on a single site  $s$ , its configurational average is therefore carried out as

$$\bar{X}_s = \sum_{Q=A,B} C_s^Q X_s^Q, \quad (2)$$

indicating that an averaged single-site quantity is a sum of contributions from the two possible occupants.

### B. Formulation of the CPA and derivation of $\bar{\mathcal{G}}^r$

Now, let us consider the Hamiltonian in the central region as follows:

$$H^C = \sum_s \frac{1}{2} M_s \dot{x}_s^C \dot{x}_s^C + \sum_{s,s'} \frac{1}{2} x_s^C K_{ss'}^C x_{s'}^C, \quad (3)$$

where  $M_s$  is a binomial random variable for the mass at site  $s$ ,  $x^C$  is the Heisenberg displacement operator in the central region, and  $K^C$  is the spring constant matrix for the central region. We take atom  $A$  to be the host lattice and atom  $B$  to be the impurity atom. We use the effective medium idea to derive the CPA. Working in the frequency domain and using the equation of motion method, with self-energy of the leads incorporated,<sup>17</sup> the inverse matrix of the full “ $x^C, x^C$ ” Green’s function is given as

$$\begin{aligned} \mathcal{G}(\omega)^{-1} &= M\omega^2 - K^C - \Sigma_L - \Sigma_R \\ &= M^A \omega^2 \mathbf{1} - K^C - \Sigma_L - \Sigma_R - \Delta M \omega^2 \\ &= M^A \omega^2 \mathbf{1} - K^C - \Sigma_L - \Sigma_R - \Sigma^{\text{CPA}} \\ &\quad - \Delta M \omega^2 + \Sigma^{\text{CPA}}, \end{aligned} \quad (4)$$

where  $\mathbf{1}$  is the identity matrix of sites and the random variable  $\Delta M_s$  is the matrix element of the diagonal matrix  $\Delta M$ , taking the value 0 when site  $s$  is occupied by atom  $A$  and the value  $M^A - M^B$  when site  $s$  is occupied by atom  $B$ . The aim of the manipulation above is to single out the terms that represent the host lattice Green’s function (with leads) and to introduce a CPA self-energy term that is understood to be a diagonal matrix with matrix elements  $\Sigma_{s,s'}^{\text{CPA}} = \Sigma_s^{\text{CPA}} \delta_{s,s'}$ . This CPA self-energy term is a frequency-dependent mean field. We let  $V_s = \Delta M_s \omega^2 - \Sigma_s^{\text{CPA}}$  and define the host lattice Green’s function (with leads) as

$$\mathcal{G}^0(\omega) = [M^A \omega^2 \mathbf{1} - K^C - \Sigma_L - \Sigma_R - \Sigma^{\text{CPA}}]^{-1}. \quad (5)$$

The full Green’s function can thus be written in the form of a Dyson equation,

$$\mathcal{G}(\omega) = \mathcal{G}^0(\omega) + \mathcal{G}^0(\omega) V \mathcal{G}(\omega), \quad (6)$$

where  $V$  is diagonal with elements  $V_s$ . Then, written in the scattering  $T$ -matrix form, the Green’s function is

$$\mathcal{G} = \mathcal{G}^0 + \mathcal{G}^0 T \mathcal{G}^0, \quad (7)$$

where  $T = V (\mathbf{1} - V \mathcal{G}^0)^{-1}$ . Since the random variables are in  $T$  only, we can take the configurational average easily:

$$\bar{\mathcal{G}} = \mathcal{G}^0 + \mathcal{G}^0 \bar{T} \mathcal{G}^0. \quad (8)$$

Since we are free to choose the term  $\Sigma^{\text{CPA}}$ , we shall make a simple approximation by choosing  $\Sigma^{\text{CPA}}$  such that  $\bar{T} = 0$ . This condition implies a simple approximation for the configuration-averaged Green’s function,

$$\bar{\mathcal{G}} = \mathcal{G}^0. \quad (9)$$

However, the condition  $\bar{T} = 0$  is still intractable for the explicit evaluation of  $\Sigma^{\text{CPA}}$ . Thus, we make further approximations to the  $T$  matrix. Define a single-site  $T$  matrix  $t_s$  as a matrix of all zero elements except at the  $(s, s)$  entry, where it takes the value

$$t_s = \frac{V_s}{1 - V_s \mathcal{G}_{ss}^0}. \quad (10)$$

Expanding and iterating the Dyson equation in terms of  $t_s$  and comparing with the  $T$ -matrix equation, we get

$$T = \sum_s t_s + \sum_s \sum_{s' \neq s} t_s \mathcal{G}_{ss'}^0 t_{s'} + \sum_s \sum_{s' \neq s} \sum_{s'' \neq s'} t_s \mathcal{G}_{ss'}^0 t_{s'} \mathcal{G}_{s's''}^0 t_{s''} + \dots \quad (11)$$

We now take the configurational average and apply the single-site approximation (SSA) to the above equation to decouple the single-site scattering in the coupled equation, as follows:

$$\bar{T} \approx \sum_s \bar{t}_s + \sum_s \sum_{s' \neq s} \bar{t}_s \mathcal{G}_{ss'}^0 \bar{t}_{s'} + \sum_s \sum_{s' \neq s} \sum_{s'' \neq s'} \bar{t}_s \mathcal{G}_{ss'}^0 \bar{t}_{s'} \mathcal{G}_{s's''}^0 \bar{t}_{s''} + \dots \quad (12)$$

From the condition  $\bar{T} = 0$ , which now simplifies to  $\bar{t}_s = 0$ , we obtain the self-consistent relation

$$0 = C_s^A \frac{-\Sigma_s^{\text{CPA}}}{1 + \Sigma_s^{\text{CPA}} \mathcal{G}_{ss}^0} + C_s^B \frac{(M^A - M^B)\omega^2 - \Sigma_s^{\text{CPA}}}{1 - [(M^A - M^B)\omega^2 - \Sigma_s^{\text{CPA}}] \mathcal{G}_{ss}^0}. \quad (13)$$

This is the phonon analog of Eq. (3.22b) in the review paper Ref. 4. As shown in the review paper,<sup>4</sup> we can put it into a form symmetric in atom  $A$  and atom  $B$ . We can also think of the CPA self-energy as introducing a frequency-dependent effective mass,  $\mathcal{M}_s$  which is defined by  $\Sigma_s^{\text{CPA}} = (M^A - \mathcal{M}_s)\omega^2$ . By rewriting Eq. (13) in terms of  $\mathcal{M}_s$ , we get the above-mentioned symmetric form,

$$\mathcal{M}_s = \bar{M} + (\mathcal{M}_s - M^A) \mathcal{G}_{ss}^0 (\mathcal{M}_s - M^B) \omega^2, \quad (14)$$

where  $\bar{M} = C_s^A M^A + C_s^B M^B$ . For retarded (superscript  $r$ ) and advanced (superscript  $a$ ) functions, we simply replace  $\omega^2$  with  $(\omega + i\eta)^2$  and  $(\omega - i\eta)^2$ , respectively.

### C. Average transmission coefficient: nonequilibrium vertex correction

The previous subsection illustrates the (frequency-dependent) mean field approximation used in calculating the (approximate) configuration-averaged Green's function. However, in calculating the configuration-averaged thermal conductance,  $\sigma$  [Eq. (137) in Ref. 16], we need to configuration average the Caroli formula [=  $\text{Tr}(\mathcal{G}^r \Gamma_L \mathcal{G}^a \Gamma_R)$ , see also Eq. (57) in Ref. 16], i.e.,

$$\sigma = \int_0^\infty \frac{d\omega}{2\pi} \hbar \omega \text{Tr}(\overline{\mathcal{G}^r \Gamma_L \mathcal{G}^a \Gamma_R}) \frac{\partial f}{\partial T}, \quad (15)$$

where  $f$  is the Bose-Einstein distribution and  $\Gamma_{L,R} = i(\Sigma_{L,R}^r - \Sigma_{L,R}^a)$ . The configuration averaging of the Caroli formula involves a product of two Green's functions (with other nonrandom terms), this is known as vertex correction in diagrammatic many-body field theory.

We shall evaluate the vertex correction in the spirit of the CPA. Inserting  $\mathcal{G}^r = \mathcal{G}^{0r} + \mathcal{G}^{0r} T^r \mathcal{G}^{0r}$  and  $\mathcal{G}^a = \mathcal{G}^{0a} + \mathcal{G}^{0a} T^a \mathcal{G}^{0a}$  into the averaged Caroli formula, and using the

CPA condition  $\bar{T}^r = 0 = \bar{T}^a$ , we obtain

$$\text{Tr}(\overline{\mathcal{G}^r \Gamma_L \mathcal{G}^a \Gamma_R}) = \text{Tr}(\overline{\mathcal{G}^r \Gamma_L \mathcal{G}^a \Gamma_R}) + \text{Tr}(\overline{\mathcal{G}^r \Omega_{\text{NVC}} \mathcal{G}^a \Gamma_R}), \quad (16)$$

where we have defined the nonequilibrium vertex correction matrix  $\Omega_{\text{NVC}}$  as

$$\Omega_{\text{NVC}} = \overline{T^r \mathcal{G}^r \Gamma_L \mathcal{G}^a T^a}. \quad (17)$$

We apply SSA and the CPA condition to further simplify  $\Omega_{\text{NVC}}$ . For details, see the supplemental document accompanying Ref. 6. After the simplification, we can find that  $\Omega_{\text{NVC}}$  is actually a site-diagonal matrix

$$\Omega_{\text{NVC}} \approx \sum_s \Omega_{\text{NVC},s} = \sum_s \overline{\Lambda_s^r \mathcal{G}^r \Gamma_L \mathcal{G}^a \Lambda_s^a}, \quad (18)$$

where  $\Lambda_s^{r,a} = t_s^{r,a} (1 + \mathcal{G}^{r,a} \sum_{s'(\neq s)} \Lambda_{s'}^{r,a})$ . Applying the SSA to  $\Omega_{\text{NVC},s}$ , we decouple the average of  $t_s^r$  and  $t_s^a$  with  $s = s'$  in pairs and we can find that it satisfies a self-consistent equation:

$$\Omega_{\text{NVC},s} = \overline{t_s^r \mathcal{G}^r \Gamma_L \mathcal{G}^a t_s^a} + \overline{t_s^r \mathcal{G}^r \sum_{s' \neq s} \Omega_{\text{NVC},s'} \mathcal{G}^a t_s^a}. \quad (19)$$

Since the quantity in the above equation is the average over a single-site quantity, it can be rewritten as a sum of contributions from each species:

$$\Omega_{\text{NVC},s} = \sum_{Q=A,B} C_s^Q t_s^{Q,r} \mathcal{G}^r \Gamma_L \mathcal{G}^a t_s^{Q,a} + \sum_{Q=A,B} C_s^Q t_s^{Q,r} \mathcal{G}^r \sum_{s' \neq s} \Omega_{\text{NVC},s'} \mathcal{G}^a t_s^{Q,a}. \quad (20)$$

### III. TEST RUNS AND COMPARISON

Based on the formalism given in the previous section, we shall evaluate the configuration-averaged thermal conductance  $\sigma$ . The procedure is as follows: solve the self-consistent

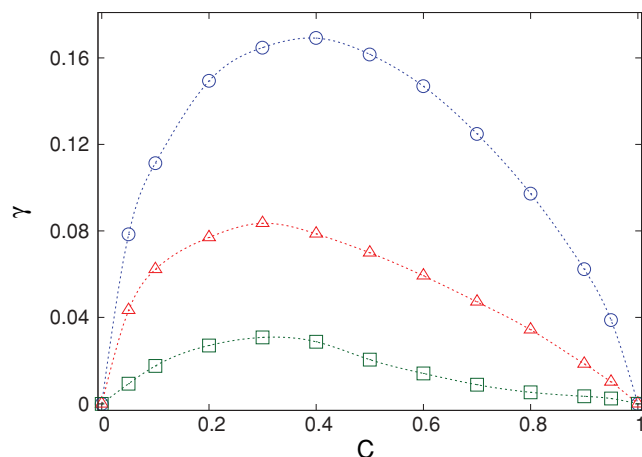


FIG. 1. (Color online) Difference  $\gamma$  of the thermal conductances between the exact brute-force results and the numerical solutions of the theory, defined as  $\gamma = |\sigma_{\text{CPA}} - \sigma_{\text{exact}}|/\sigma_{\text{exact}}$ , for three- (circles), five- (triangles) and seven-atom (squares) 1D harmonic atomic chains of  $M^A = 1$  doped with impurities of  $M^B = 2$ . The whole concentration range is varied and the values are taken at room temperature (300 K).

equation (13) to get  $\Sigma^{\text{CPA}}$ , then evaluate the configuration-averaged Green's function by using (5) [this is due to (9)], then  $t_s$  is evaluated from (10), and so  $\Omega_{\text{NVC},s}$  can be evaluated from the self-consistent equation (20). Finally, the conductance is calculated using (16) and then (15). Figure 1 is a plot of the percentage difference  $\gamma$  between the numerical solutions and the exact brute-force results on one-dimensional atomic chains of  $M^A = 1$  doped with impurities of  $M^B = 2$ . The latter is calculated by averaging the coefficients over all possible configurations of the system. We can tell that although the numerical solutions give us slightly smaller values (which is expected since the CPA is an undercorrection), even for a small system containing only three atoms, the error is less than 20%. For a system containing five atoms, the error is reduced to less than 10%, and when the system size increases to seven atoms, the error is within 3%. This verifies that this method is very accurate to describe relatively large systems. After these cross-checks, we can confidently proceed to apply it to the topic that attracts a lot of attention—the isotopic disorder effect on the thermal transport behavior in harmonic chains and carbon nanotubes.

#### IV. ONE-DIMENSIONAL DISORDERED HARMONIC CHAINS

The method is first employed to study the heat conduction in disordered harmonic chains with atomic mass  $M^A = 1$  and isotopic mass  $M^B = M$ . This problem has attracted a lot of attention for almost 30 years.<sup>9–11,18–20</sup> One main issue here is to determine the dependence of the thermal conductivity  $\kappa$  defined as  $\kappa = \sigma N$ , where  $\sigma$  is the thermal conductance, on system size  $N$ . A large number of studies<sup>9–12</sup> suggest that, in one dimension, Fourier's law may be violated in the form of  $\kappa \sim N^\alpha$ , with  $0 < \alpha < 1$ . The most important argument is that the exponent  $\alpha$  depends on the properties of the heat baths.<sup>11</sup> Here, it is proved again in Fig. 2, for the Rubin-Greer model,<sup>9</sup> where the surface Green's function takes the form  $\frac{1}{2}(2 - \omega^2 + i\omega\sqrt{4 - \omega^2})$ , the exponent  $\alpha$  is 1/2, which is exactly the value of the slope of the upper line in Fig. 2. Furthermore, we test the sensitivity of the heat bath dependence on  $\kappa$ . We first add a small enough  $10^{-5}$  on-site potential to each atom in the heat baths. This causes the vanishing of the low-frequency part of the transmission coefficient, which leads to a turning point of the exponent  $\alpha$ . We then restrict this small on-site potential to only the first and last atoms in the center by simply adding in an imaginary part  $\eta = 10^{-5}$  to the frequency  $\omega$  in Rubin's model, and the self-energy of the leads has the small-expansion form of  $1 - \eta + O(\omega)$ . The low-frequency phonons survive in this case, but the turning point is still present, although it appears at a much larger  $N$ . The positions of the turning points can also be affected<sup>20</sup> by  $M$  and this length scale can be fitted with  $\frac{1}{\sqrt{M\eta}}$ . Therefore, even slight changes that break the translational invariance of the central system lead to the reduction of the low-frequency part in the transmission coefficient and consequently a change in the power law. This evidence confirms the previous statements<sup>11,20</sup> that the major contribution to the exponent  $\alpha$  comes from the low-frequency phonons. However, the authors of Refs. 11 and 20 also indicated cases where the exponent  $\alpha$  may not

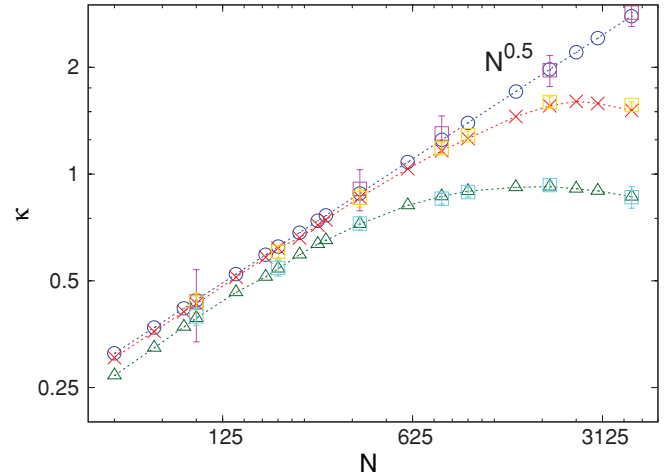


FIG. 2. (Color online) Thermal conductivity of one-dimensional disordered harmonic chains of  $M^A = 1$  doped with impurities of  $M^B = 50$  and concentration  $C = 40\%$  at room temperature (300 K), plotted in log-log scale: from top to bottom, disordered chain (calculated with the CPA) with free-boundary conditions (circles), disordered chain (calculated with the CPA) with only the first and last atom in the center added with a  $10^{-5}$  on-site potential (crosses), and disordered chain (calculated with the CPA) with all the atoms in the leads added with a  $10^{-5}$  on-site potential (triangles). Monte Carlo simulations of the same systems are also plotted for comparison (squares with error bars).

be a constant for the same type of heat bath and for a fixed number of pinning centers. The exponent value indeed varies with different system sizes. We also performed Monte Carlo experiments to check all these three cases. Different configurations are generated according to their probabilities. For example, if we assume that the concentration of impurities is  $C$ , then the probability of obtaining the configuration with  $n$  impurities over  $N$  sites is  $\binom{N}{n}(1 - C)^{N-n}C^n$ . The experiments are realized by averaging the conductivities from each generated configuration. The two methods agree with each other very well.

#### V. EFFECT OF ISOTOPE DISORDER ON CARBON NANOTUBES

Now we apply the theory to (5,5) carbon nanotubes of different lengths, and let  $^{14}\text{C}$  be a random dopant in the pure  $^{12}\text{C}$  environment. Force constant matrices are obtained from the Brenner empirical potential as implemented in the “General Utility Lattice Program” (GULP).<sup>21</sup> Figure 3(a) shows the relation between averaged thermal conductance  $\sigma$  and the concentration  $C$  of the dopant  $^{14}\text{C}$ . For the short length around 1 nm, the resistance between leads and central part plays a more important role, while the effects due to isotope disorder are minor. However, when the length of the nanotube is longer, scattering due to isotope disorder dominates the transport properties, where the largest reduction of thermal conductance happens when the concentration is around 50%. Because of the lack of disorder scattering, the conductance values in the two extreme cases of concentration are the same regardless of the length of the nanotube. The thermal conductivity  $\kappa$

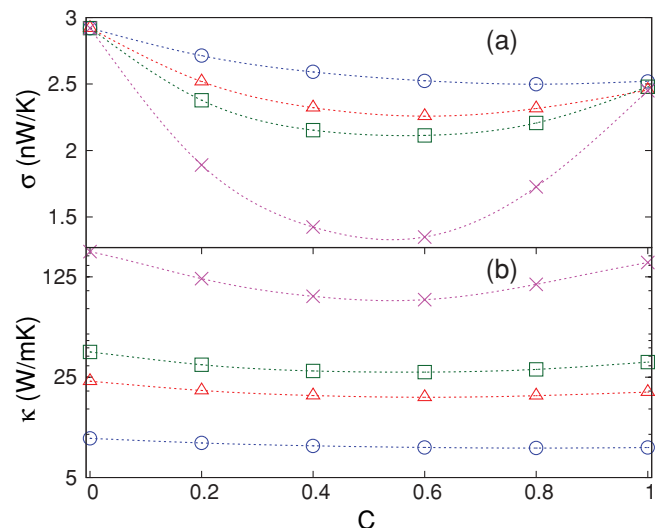


FIG. 3. (Color online) Thermal transport properties of carbon nanotubes with different lengths at room temperature (300 K): 0.9 (circles), 2.46 (triangles), 3.94 (squares), and 19.68 nm (crosses). (a) The thermal conductance  $\sigma$  of  $^{12}\text{C}$  nanotubes doped with different concentrations of  $^{14}\text{C}$ . (b) The thermal conductivity  $\kappa$  of  $^{12}\text{C}$  nanotubes doped with different concentrations of  $^{14}\text{C}$ .

of doped carbon nanotubes is plotted in Fig. 3(b). It is calculated from  $\sigma L/S$ , where  $L$  is the tube length and  $S$  is the cross-sectional area of the tube. We choose  $d = 1.44 \text{ \AA}$  as the tube thickness; thus, the cross section is  $2\pi r d$ , where  $r$  is the radius of the tube. Comparing over different lengths of nanotubes, one can tell that, as the length becomes longer, the proportional reduction of thermal conductance increases. For the nanotube around 20 nm long, isotope disorder can reduce the thermal conductance by approximately 50%, which agrees with a previous classical molecular dynamics simulation<sup>14</sup> and the experimental results<sup>15</sup> on isotopically doped boron nitride nanotubes.

We shall now consider the modification of the divergent behavior due to disorder scattering. The thermal conductivity of 40% doped carbon nanotubes vs their lengths is plotted

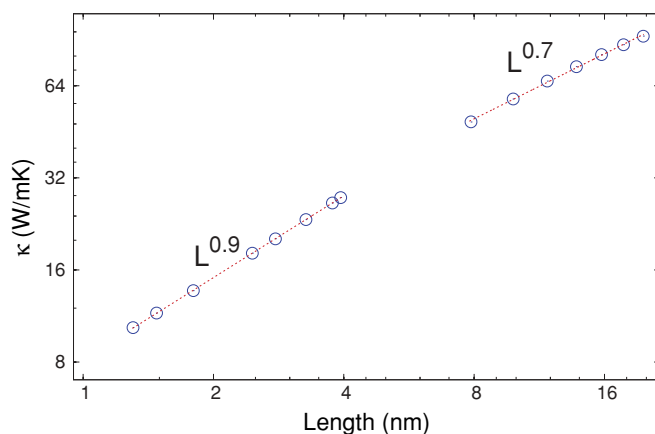


FIG. 4. (Color online) The thermal conductivity of carbon nanotubes vs their lengths at room temperature (300 K) with doping concentration 40%. The dashed line represents the fitting results for different length scales.

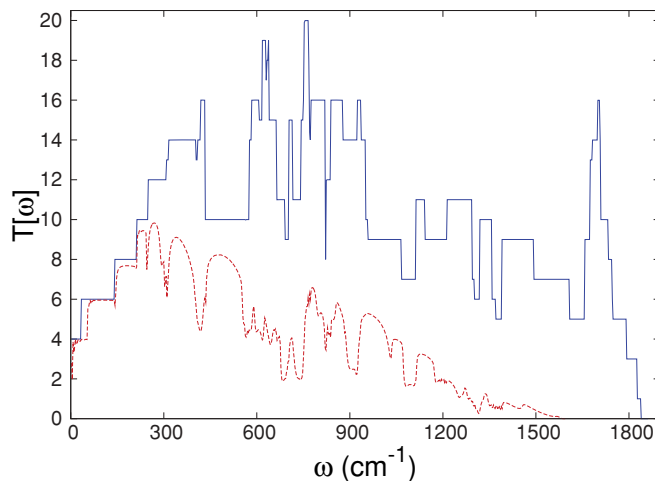


FIG. 5. (Color online) The transmission coefficient of a perfect infinite (5,5) carbon nanotube (solid line) and that of a nanotube of length 11.8 nm with  $^{14}\text{C}$  doped at the concentration of 40% (dashed line).

in Fig. 4. The fitting line in the figure clearly shows the change in its divergent behavior: when the length of the carbon nanotube is within 4 nm, the conductivity varies with the length as  $\kappa \sim L^{0.9}$ , and when the length of the carbon nanotube is longer than 8 nm, the exponent changes from 0.9 to 0.7. This range is consistent with the experimental results in Ref. 22 where the authors found the exponent to be between 0.6 and 0.8. However, it seems as if our numerical results show a “transition” in divergent behavior. We suggest that the transition in divergent behavior could be due to the change in relative weights of the frequency spectrum as the length of the nanotube changes. The argument for our suggestion is as follows: We are working with a harmonic system with independent modes so that phonon–phonon interaction is excluded, and we think that different modes would contribute to the divergent behavior differently and, with the fact that the length affects the weights of the frequency spectrum, we suspect that the change in relative weights is the reason behind the transition. This is an important area for further numerical and theoretical investigations.

The phonon transmission coefficient of a perfect infinite carbon nanotube and that of an isotopically doped carbon nanotube are compared in Fig. 5, where the dramatic reduction effect due to the localization of high-frequency modes is clearly shown, and the longer the carbon nanotube is, the larger the proportion of high-frequency modes not contributing to transmission. We can also see from Fig. 5 that high-frequency phonons are localized preferentially over the low-frequency phonons in the presence of isotope disorder.

## VI. CONCLUSION

In conclusion, we have developed a nonequilibrium theory that can take care of the configurational averaging of thermal transport coefficients in disordered nanoscale systems. The configurational averaging is achieved approximately via the CPA. To that end, we achieved the configurational averaging of the Caroli formula by solving two self-consistent equations.

It should be noted that in the Kubo formula treatment,<sup>23</sup> where thermal conductivity is calculated from the correlation of thermal-current-density operators, due to crystal inversion symmetry, vertex correction terms vanish, whereas in this paper, vertex corrections entering the Caroli formula do not vanish under crystal inversion symmetry. The accuracy of this theory is then tested with exact results and with Monte Carlo experiments on one-dimensional disordered harmonic chains, and the suitability of this method in handling relatively large systems is shown. The previously proposed power law form of thermal conductivity has been recovered and we also indicate the possibility of varying the exponent for larger system size. We applied our method to the quantum thermal transport in carbon nanotubes. Anomalous thermal transport has been shown and we also observe the transition

between different transport regimes due to the scattering of phonons by impurities. This effect reduces the thermal conductance of carbon nanotubes, which verifies doping as a feasible way of manipulating the performance of nanodevices, especially in applications that make use of thermoelectricity. Therefore, this proposed method can be widely used because it provides relatively accurate results but requires only a one-time calculation rather than thousands of repeated calculations in the brute-force method for predicting quantum thermal transport properties of disordered nanoscale systems.

#### ACKNOWLEDGMENT

J.-S.W. is supported in part by Research Grant No. R-144-000-257-112 from National University of Singapore.

- 
- <sup>1</sup>R. Rurali, T. Markussen, J. Sune, M. Brandbyge, and A.-P. Jauho, *Nano Lett.* **8**, 2825 (2008).  
<sup>2</sup>N. Yang, G. Zhang, and B. Li, *Nano Lett.* **8**, 276 (2008).  
<sup>3</sup>E. Y. Tsybal, A. Sokolov, I. F. Sabirianov, and B. Doudin, *Phys. Rev. Lett.* **90**, 186602 (2003).  
<sup>4</sup>R. J. Elliott, J. A. Krumhansl, and P. L. Leath, *Rev. Mod. Phys.* **46**, 465 (1974).  
<sup>5</sup>F. Yonezawa and K. Morigaki, *Prog. Theor. Phys. Suppl.* **53**, 1 (1973).  
<sup>6</sup>Y. Ke, K. Xia, and H. Guo, *Phys. Rev. Lett.* **100**, 166805 (2008).  
<sup>7</sup>M. O. Robbins and B. Koiller, *Phys. Rev. B* **27**, 7703 (1983).  
<sup>8</sup>R. Vlaming and D. Vollhardt, *Phys. Rev. B* **45**, 4637 (1992).  
<sup>9</sup>R. Rubin and W. Greer, *J. Math. Phys. (NY)* **12**, 1686 (1971).  
<sup>10</sup>A. J. O'Connor and J. L. Lebowitz, *J. Math. Phys. (NY)* **15**, 692 (1974).  
<sup>11</sup>A. Dhar, *Phys. Rev. Lett.* **86**, 5882 (2001).  
<sup>12</sup>B. Li, J. Wang, L. Wang, and G. Zhang, *Chaos* **15**, 015121 (2005).  
<sup>13</sup>D. Roy and A. Dhar, *Phys. Rev. E* **78**, 051112 (2008).  
<sup>14</sup>G. Zhang and B. Li, *J. Chem. Phys.* **123**, 114714 (2005).  
<sup>15</sup>C. W. Chang, A. M. Fennimore, A. Afanasiev, D. Okawa, T. Ikuno, H. Garcia, D. Li, A. Majumdar, and A. Zettl, *Phys. Rev. Lett.* **97**, 085901 (2006).  
<sup>16</sup>J.-S. Wang, J. Wang, and J. T. Lü, *Eur. Phys. J. B* **62**, 381 (2008).  
<sup>17</sup>T. Yamamoto and K. Watanabe, *Phys. Rev. Lett.* **96**, 255503 (2006).  
<sup>18</sup>V. N. Likhachev, G. A. Vinogradov, T. Yu. Astakhova, and A. E. Yakovenko, *Phys. Rev. E* **73**, 016701 (2006).  
<sup>19</sup>A. Chaudhuri, A. Kundu, D. Roy, A. Dhar, J. L. Lebowitz, and H. Spohn, *Phys. Rev. B* **81**, 064301 (2010).  
<sup>20</sup>H. Matsuda and K. Ishii, *Prog. Theor. Phys. Suppl.* **45**, 56 (1970).  
<sup>21</sup>J. Gale, *J. Chem. Soc., Faraday Trans.* **93**, 629 (1997).  
<sup>22</sup>C. W. Chang, D. Okawa, H. Garcia, A. Majumdar, and A. Zettl, *Phys. Rev. Lett.* **101**, 075903 (2008).  
<sup>23</sup>J. K. Flicker and P. L. Leath, *Phys. Rev. B* **7**, 2296 (1973).